Available online at www.sciencedirect.com
ScienceDirect
Catalysis Today 118 (2006) 63–72
CATALYSIS TODAY
www.elsevier.com/locate/cattod

Studies of self-supported 1.6 μm Pd/23 wt.% Ag membranes during and after hydrogen production in a catalytic membrane reactor

B. Arstad [a], H. Venvik [b,*], H. Klette [c], J.C. Walmsley [a], W.M. Tucho [d], R. Holmestad [d], A. Holmen [b], R. Bredesen [c]

[a] *SINTEF Materials and Chemistry, 7465 Trondheim, Norway*
[b] *Department of Chemical Engineering, Norwegian University of Science and Technology (NTNU), Sem Sælands vei 4, NO-7491 Trondheim, Norway*
[c] *SINTEF Materials and Chemistry, 0314 Oslo, Norway*
[d] *Department of Physics, NTNU, 7491 Trondheim, Norway*

Available online 11 July 2006

Abstract

Water-gas shift (WGS) and methanol steam reforming (MSR) were performed in a catalytic membrane reactor configuration using self-supported Pd/23 wt.% Ag membranes of 1.6 μm thickness. A commercial Cu/ZnO/support catalyst was used. Effects on hydrogen permeation and membrane stability were investigated under the application of relevant conditions. The membranes were studied with X-ray photoelectron spectroscopy (XPS) and transmission electron microscopy (TEM) before and after usage to characterize the surface composition, microstructure and texture. The self-supported membrane configuration allows exploration of the membrane bulk and surface effects without any influence of a porous support. The extremely low membrane thickness means a greater influence of surface processes compared to thicker membranes.

Keywords: Water-gas shift; Palladium; Methanol steam reforming; Membrane reactor

1. Introduction

Considerable interest has been expressed in recent years in the use of catalytic membrane reactors [1]. These systems offer increased efficiency and compactness, since they combine both reaction (catalytic) and separation (membrane) operations in a single unit. The membrane can be used to add a reactant or selectively remove a product species. With proper reactor design, the product extraction from the reaction zone may facilitate a shift in the reaction equilibrium towards the product side. As a result, higher conversion and yields can be attained.

An important application for catalytic membrane reactors involves the removal or addition of hydrogen by using membranes made of palladium (Pd) or palladium alloys [1]. Recently, an extensive review on palladium membrane research was published by Paglieri and Way [2]. Another relevant overview article on membrane catalysis was published by Armor in 1995 [3].

Pd has considerable solubility for hydrogen and absorbs about 600 times its volume of hydrogen at room temperature [1]. However, Pd undergoes a phase transition between the α- and β-phases near room temperature when exposed to hydrogen [3]. This makes the materials brittle and eventually leads to micro-cracks in the metal. To avoid this problem, one has to operate above 300 °C where the β-phase is absent [3]. The phase change problem can be considerably reduced by employing various Pd alloys. By alloying Pd with 1–30% Ag, Rh or Ru, the β-phase is absent above approximately 77 °C [3]. Pd/Cu alloys exhibit similar resistance to the α- and β-phase change as the Pd/Ag alloys [2]. Pd alloyed with Ag or Cu can have hydrogen permeation rates that surpass pure Pd, and in addition the mechanical strength of these alloys is significantly improved compared to pure Pd [1,2]. Optimum compositions of Pd–Ag and Pd–Cu alloys have been found to be ∼23 wt.% and

* Corresponding author. Tel.: +47 73592831; fax: +47 73594080.
E-mail address: hilde.venvik@chemeng.ntnu.no (H. Venvik).

0920-5861/$ – see front matter
doi:10.1016/j.cattod.2006.01.041

~40 wt.%, respectively. A mechanically flawless Pd-based membrane shows 100% selectivity towards hydrogen permeation.

From a technological point of view, a catalytic membrane reactor system for hydrogen production could for example be implemented in a mobile unit for power generation via a fuel cell. A compact membrane reactor unit with 100% hydrogen separation selectivity could be particularly suited to feed low temperature proton exchange membrane fuel cells (PEMFC), since these have high requirements with respect to contamination from for example CO.

Hydrogen can be produced from hydrocarbons or oxygenates via a single or a series of catalytic reactions. Two important reactions proceeding in the range 200–500 °C and over similar catalysts are the water-gas shift (WGS) and methanol steam reforming (MSR) reactions:

$$CO(g) + H_2O(g) \leftrightarrow CO_2(g) + H_2(g), \Delta H_{298\,K} = -41.3\,kJ/mol \quad (1)$$

$$CH_3OH(g) + H_2O(g) \leftrightarrow CO_2(g) + 3H_2(g), \Delta H_{298\,K} = +49.4\,kJ/mol \quad (2)$$

For both reactions CO is usually present in the product stream. During WGS (1), CO originates from unconverted reactants, whereas for MSR (2), CO can form via the reverse water-gas shift reaction or by direct decomposition of methanol.

Other research groups have also reported on WGS [4–9] or MSR [10–15] reactions in Pd-based catalytic membrane reactors. Recent reports on hydrogen production/separation in catalytic membrane reactors include dehydrogenation of alcohols such as ethanol [16–18] or butanol [19] and dehydrogenation of alkanes such as ethane [20–23], propane [24–27], isobutane [27–32], cyclohexane [33–35] or methylcyclohexane [36,37]. Steam reforming of methane has also been reported for hydrogen production in membrane reactors [38–43].

In the present work, we report on the performance and stability of 1.6 μm self-supported Pd/23 wt.% Ag membranes during WGS and MSR reactions. Transmission electron microscopy (TEM) and X-ray photoelectron spectroscopy (XPS) were used to characterize both unused and used membranes.

2. Experimental

Pd/Ag thin films were deposited by magnetron sputtering on a silicon substrate to 1.6 μm thickness, using a Pd/23 wt.% Ag target [44]. After fabrication, a piece of the metallic foil of suitable size could be lifted off the substrate and sealed between two steel plates, each with a 17.5 mm drilled hole. The membrane surface area of each experiment was thus 2.40 cm^2. This configuration was mounted in a metal housing and tested for leaks with He to ensure that each membrane had no pinholes and was perfectly dense. Two Pd/23 wt.% Ag membrane units were prepared for the present work; one for WGS and one for MSR experiments. The side of the membrane originating from the silicon–Pd/Ag interface was kept facing the permeate side in all experiments.

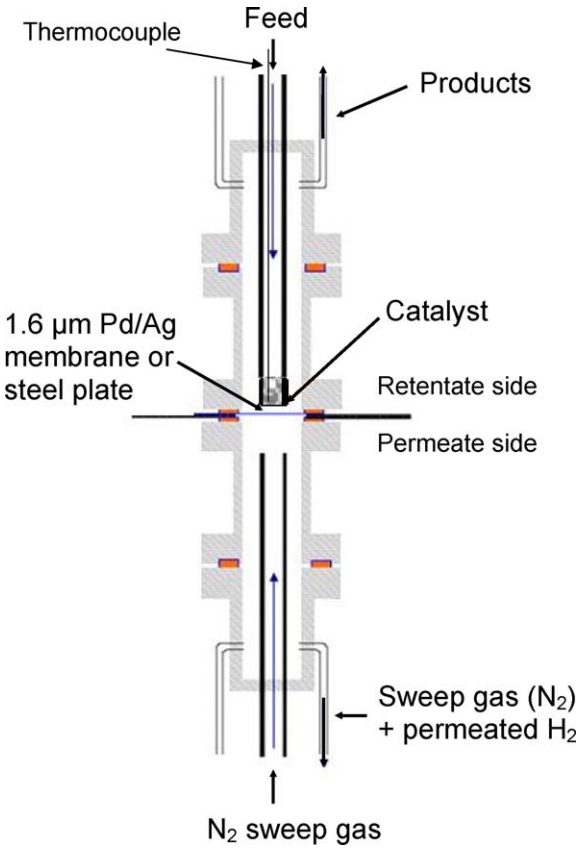

Fig. 1. Schematic drawing of the membrane reactor configuration.

The reactor is a fixed-bed type with the catalyst bed located 2–3 mm above the self-supported membrane. Fig. 1 contains a sketch of the membrane reactor configuration. The thermocouple was located in the catalyst bed. The difference between the furnace set-point temperature and the measured temperature in the catalyst bed was ~10 °C, and was observed not to change between exothermic (WGS), endothermic (MSR) and non-catalytic experiments (H_2 permeation). All temperatures given in this text are thus measured in the position of the catalyst bed, ~3 mm above the membrane. A commercial methanol synthesis catalyst, Cu/ZnO/support, was used in all reaction experiments. Catalyst (0.30 g) of 400–630 μm particle size was mixed with 1.00 g, 300 μm SiC particles, resulting in a ca. 15 mm long catalyst bed. The catalyst was reduced at 220 °C for 3 h in pure hydrogen at 100 NmL/min (0 °C, 1 atm).

Permeation and reaction experiments were performed in the range 190–275 °C using the feed and sweep gas flow rates specified in Table 1. Mass flow controllers were applied to regulate both gaseous and liquid flows. The liquid was fed into an evaporator and subsequently mixed with the gases. The total pressure was close to ambient, and the pressure difference across the membrane was 0.01–0.02 bar, with the highest pressure on the retentate side. A constant flow of nitrogen was used as sweep gas in all experiments. Between the experiments, nitrogen was flushed through the membrane reactor on both

Table 1
Feed and sweep gas flow rates (NmL/min) in pure hydrogen permeation experiments (1), with Y (Y = CO/H_2O/N_2) separately added (2), water-gas shift (3), and methanol steam reforming (4) reaction experiments, as well as during inert flushing (5) between experiments

Feed	(1) H_2 pure	(2) H_2 + Y	(3) WGS	(4) MSR	(5) N_2 flush
H_2	100 + (25)	100			
CO		(25)	50	–	
H_2O		(25)	100	40	
N_2		(25)	–	40	25
MeOH			–	20	
N_2 sweep	50	50	50	50	25

permeate and retentate sides at 190 °C. The time period ranging from the first to the last day of either a WGS or a MSR experiment carried out over a particular membrane is referred to as the WGS or MSR experimental period. Note that WGS/MSR experiments were not carried out for all the days within the experimental period, and that each membrane was subjected to either WGS or MSR reaction conditions only. Reaction experiments carried out in the reactor with a steel plate installed in place of the Pd/Ag membrane will be referred to as ''using a plate'' or analogous expressions. With a plate mounted, the configuration resembles a conventional fixed-bed reactor. Dry gas analyses of H_2, CO, CO_2, N_2 and trace CH_4 were conducted for both permeate and retentate flows using an Agilent 3000 Micro GC.

The hydrogen permeation capacity and the membrane deactivation were investigated by feeding pure hydrogen on the retentate side (Table 1), and measuring the amount of H_2 permeated through the membrane. The total pressure was 1.06 bar on the retentate side and 1.05 bar on the permeate side. In these experiments, the hydrogen partial pressure over the membrane would be approximately 0.5 bar. The experiments usually took place over several hours to obtain a steady-state hydrogen permeation, and were carried out prior to, and during the WGS and MSR experimental periods. For the permeation experiments carried out prior to the reaction experiments, the temperatures ranged from 185 °C to 270 °C. During the WGS and MSR experimental periods, pure hydrogen permeation experiments were carried out at 255 °C only.

The individual effect of N_2, CO or H_2O (steam) on the H_2 permeation rate was also investigated over the WGS membrane, prior to any WGS experiments, to obtain a general impression of a possible negative effect of different gases on the membrane performance in our reactor. N_2, CO or H_2O was added to the reactant mixture at 255 °C after a steady-state H_2 flow through the membrane of approximately 50 NmL/min was reached.

WGS reaction experiments were conducted feeding CO and steam at a ratio of 1:2 without any inert gases added (Table 1). For the MSR experiments, a binary solution of methanol and water was prepared. The solution was evaporated and subsequently mixed with nitrogen to obtain a 1:2:2 (mole fraction) reactant gas mixture of methanol, steam and N_2 (Table 1).

The last experiments carried out before dismounting the membranes for characterization were WGS and MSR reactions. XPS of the membranes was performed using a hemispherical SCIENTA SES 2002 electron analyser (Gammadata Scienta). A monochromatized Al Kα source (GammaData Scienta) provided the X-rays. The energy resolution is estimated to 0.6 eV. Pd 3d, Ag 3d, C 1s and O Auger signals were used for quantification. O Auger was used for quantification because the O 1s peak overlapped with the Pd $3p_{3/2}$ peak.

TEM investigations were carried out using a Philips CM 30 at 300 kV accelerating voltage. Cross-section samples were prepared from Pd/Ag membranes subjected to either WGS or MSR reaction experiments. Monocrystalline silicon strips were used for supporting the foils in the cross-section samples. The silicon strip facing the permeate side was coated with gold to easily separate it from the feed side of the foil.

3. Results and discussion

3.1. Hydrogen permeation experiments

Table 2 shows the steady-state H_2 permeation rates for the as-prepared membranes, i.e. before exposure to WGS or MSR reactant/product mixtures. These measurements will be used as reference for later deactivation tests of the membranes. Hydrogen permeation rate measurements carried out between reaction experiments during the WGS or MSR experimental periods will be reported below. Table 2 confirms that the permeation is temperature dependent. This is expected for the bulk transport. Surface desorption of hydrogen can, however, be facilitated at elevated temperature, particularly at increasing coverage. Apparently, the increasing rate of dissociation and transport of hydrogen into the bulk limits such desorption. The time to reach the maximum, steady-state flux through the membranes is considerable at the lowest temperature, whereas there is no delay at the highest temperature. This indicates that an accommodation of the Pd/Ag structure is needed to facilitate the increased transport.

By increasing the feed flow rate of pure hydrogen from 100 NmL/min to 125 NmL/min (255 °C), the hydrogen transport through the membrane is increased from 50 NmL/min, by 11 NmL/min, up to 61 NmL/min. This experiment indicates a fairly high total hydrogen flux capacity through the membrane. The hydrogen partial pressure difference over the membrane actually decreases in this experiment, since the pressure at the retentate side is not increased with increasing flow rate. It is thus the transport from the bulk of the gas to the membrane surface that is improved upon increasing the flow rate. The obtained flux data point to the importance of

Table 2
Steady-state hydrogen flow (NmL/min) through the 1.6 μm Pd/23 wt.% Ag membranes at different temperatures, with the corresponding time (t) to reach a constant hydrogen permeation

T (°C)	H_2 perm (NmL/min)	t (h)
185	40.4	∼9
255	49.4	∼1
270	49.6	∼0

Feed flow, 100 NmL/min H_2; sweep, 50 NmL/min N_2.

considering both the gas phase and surface processes when planning experiments and interpreting results, particularly when the membranes are so thin that the bulk transport does not necessarily dominate.

The addition of 25 NmL/min N_2 to the flow of 100 NmL/min pure H_2 (255 °C) caused the hydrogen flow through the membrane to decrease rapidly by 17 NmL/min, to 33 NmL/min. This decrease can be ascribed to a dilution of hydrogen close to the membrane surface and not to competitive adsorption between H_2 and N_2 on the metal surface. Simulations support the assumption that nitrogen has no adsorption effect on H_2 permeation through a Pd/Ag membrane [45].

In the literature, it is reported that the presence of CO in a gas stream over a Pd-based membrane strongly reduces the hydrogen permeation rate, presumably by blocking H_2 adsorption and/or dissociation sites [45–47]. This effect was also experienced in the present work when CO was co-fed with hydrogen (255 °C), as shown in Fig. 2. A rapid drop in the hydrogen permeation rate from 50 NmL/min to 6 NmL/min was observed when CO was added. Approximately 30 min after the CO flow was switched off, the hydrogen permeation rate had increased to 47 NmL/min. After 1 h, the permeation rate had still not reached the initial value of 50 NmL/min. This observation suggests irreversible poisoning/deactivation of the membrane as carbon containing gases are reported to react on Pd surfaces to form palladium carbides [46]. However, flushing the membrane with N_2 for almost 3 days at 190 °C, restored the initial H_2 permeation rate of 50 NmL/min. There was no detectable increase in the hydrogen permeation upon N_2 flushing at 190 °C for only one night.

A possible deactivating effect of steam on the hydrogen permeation, presumably reversible, has been ascribed to water clusters, OH groups and/or O atoms on the membrane surface [46]. When 25 NmL/min of H_2O was added to the hydrogen feed gas (255 °C), the flow rate of hydrogen through the membrane was reduced by 20 NmL/min. This is 3 NmL/min more than when nitrogen was added. These data indicate that steam, with the present reactor configuration and experimental conditions, only has a minor effect on the hydrogen permeation rate through the membrane. Hou and Hughes reported that steam had a stronger deactivating effect on the hydrogen permeation than CO, using a tubular 5–6 μm thick Pd/Ag membrane supported by α-alumina at 275 °C [45]. Since we observed that CO had a significantly stronger effect as compared to steam, our results are in apparent contrast to Hou and Hughes' findings. The differences may be attributed to different materials and reactor configuration in general.

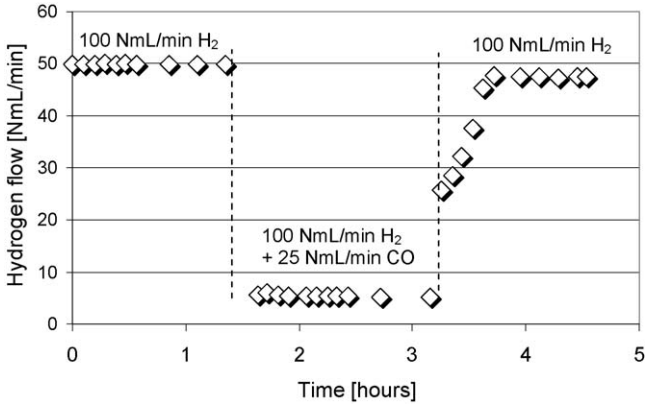

Fig. 2. The effect of CO addition on the hydrogen permeation through the membrane at 255 °C during time on stream. The dashed lines indicate the time period CO was added.

3.2. Water-gas shift reaction

To obtain regular WGS conversion data, the reactor had a metal plate mounted in place of the Pd/Ag membrane. Fig. 3 displays the product composition as a function of temperature for

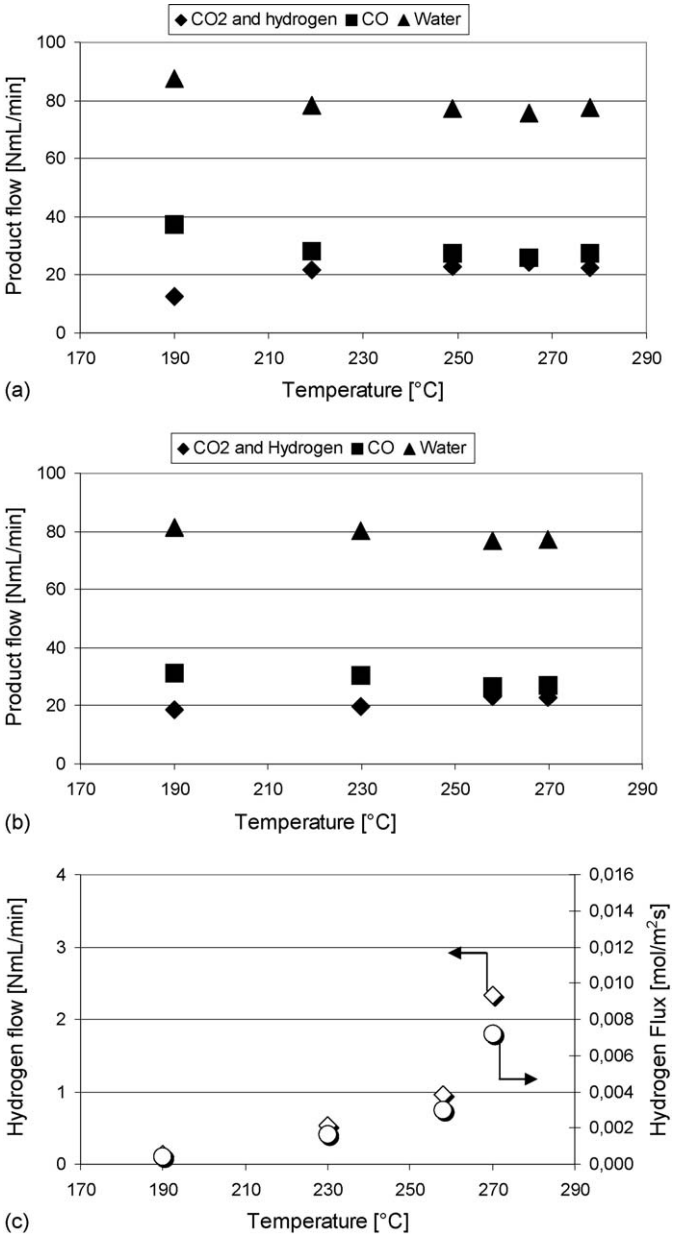

Fig. 3. Product composition (a and b) and hydrogen permeation as a function of temperature during the water-gas shift reaction: (a) WGS with plate; (b) WGS with 1.6 μm self-supported Pd/23 wt.% Ag membrane; (c) hydrogen permeation through the membrane during the experiments in (b). WGS reactant composition as specified in Table 1.

the WGS reaction over the plate (a) and the membrane (b), together with the corresponding permeation data for the membrane (c). Fig. 3(a) and (b) shows that thermodynamic equilibrium has not been reached. The thermodynamic conversion level is around ≥99% for the temperatures and reactant composition ($H_2O/CO = 2$) applied here and the conversion is thus kinetically limited, i.e. by the amount of catalyst.

The only noteworthy difference in the product composition for the WGS reaction with the Pd/Ag membrane installed (Fig. 3b) as compared to the one with the steel plate mounted (Fig. 3a) is the somewhat lower conversion at 190 °C over the steel plate. For the other temperatures, there is no significant difference in product composition with or without the membrane. These observations confirm little or no influence on the conversion by the membrane as expected under the given conditions. The primary function of the membrane is to separate hydrogen from the product gas. Studies of equilibrium shift were not an issue due to the high thermodynamic conversion level under the given conditions and with the membrane located downstream of the catalyst bed.

The hydrogen flow (NmL/min) and the corresponding flux (mol/m^2 s) through the membrane during the WGS reaction are plotted as a function of temperature in Fig. 3(c). The hydrogen flux increases relative to the CO conversion with increasing temperatures. The presence of fewer adsorbed species that are able to block hydrogen adsorption/dissociation on the Pd/Ag surface at higher temperatures may explain these observations.

The membranes may eventually deactivate due to changes in the metal structure and/or contamination/poisoning from the feed/product gas-stream under exposure to reaction conditions. Gao et al. [46] recently presented a brief review of the chemical stability of Pd-based membranes. Sulphur compounds, adsorbed CO, water, and deposited carbon from carbon containing gases are reported in literature to have poisoning and destabilizing effects [46]. The nature of the carbon containing gases is important. CO may, e.g. decompose via the Boudouard reaction ($2CO = C + CO_2$) and Collins et al. [24] reported a much stronger deactivating effect of propene as compared to propane on a Pd membrane at 550 °C. The higher propensity of alkenes over alkanes to form carbon deposits under otherwise similar conditions is well known in catalysis. For these reasons, a fundamental understanding of deactivating effects might help to improve the performance of Pd based membranes.

Table 3 reports the reduction in the hydrogen flow rate through the membrane during a period of WGS experiments. WGS experiments were carried out in the days between hydrogen permeation measurements. The H_2 permeation rate was reduced from ~50 NmL/min to ~40 NmL/min during this period of experiments. The original permeability of the membrane after WGS experiments could, however, also here be restored by keeping the membrane in N_2 at 190 °C for 3 days. As in the permeation experiments with CO added, the data indicate a slow accumulation of strongly adsorbed species that block hydrogen adsorption/dissociation which can be removed given enough time under the right conditions. It thus appears that these species relate to CO in particular, that they remain on the surface, possibly at special sites, but do not penetrate severely into the bulk. An even better identification of these species, how they form and at which sites, may point to how the membranes and the conditions can be manipulated to minimize the effect.

Table 3
Change in hydrogen permeation as measured in pure permeation experiments during the WGS reaction period over a 1.6 μm Pd/23 wt.% Ag membrane

Experimental day	WGS reaction time (*h*)	H_2 permeation (NmL/min)
1		49.6
2	6	
3		49.6
4	6	
5	6	
6	6	
7		47.5
8	6	
9	6	
10		39.6

Similarly manufactured membranes to those used in the present work could be ‘‘activated’’ by exposure to air at 300 °C over 4 days [48]. This activation procedure led to a two to three times increase in the H_2 permeation capacity. The membranes applied here were not activated in this way, in order to limit the number of parameters inflicting on the data interpretation.

3.3. Methanol steam reforming

The conversion and the product composition during the first of two MSR experiments with the same membrane mounted are shown in Fig. 4(a) and (b), respectively. As for WGS, reaction experiments with the steel plate mounted in place of the membrane were carried out first. These results (not shown) were very similar to those of Fig. 4(a), the conversion being marginally lower without the membrane. Also for this reaction we are operating in the kinetic regime. During the MSR experimental period, the methanol conversion and product compositions were reproducible from one experiment to the next. There was no deactivation of the catalyst during the experimental period. From these observations it can again be concluded that the membrane does not enhance the reaction towards the product side. The amount of CO in the product effluent is small (~<0.7–0.8 NmL/min) and more or less constant at all temperatures. The observed CO may originate from the direct decomposition of methanol and/or the reverse water-gas shift reaction.

The hydrogen flow and corresponding flux through the membrane during the MSR membrane reactor experiment reported in Fig. 4 are given in Fig. 5(a), together with comparable permeation data from the last MSR experiment over the same membrane Fig. 5(b). The initial hydrogen permeation in Fig. 5(a) was very low below 255 °C. There was no permeation at 190 °C. Since the amount of CO in the effluent gas was low, the strong reduction in hydrogen permeation is probably an effect of unconverted methanol. Hou and Hughes [45] reported that even small amounts of methanol in the hydrogen feed reduced the hydrogen permeation rate through a Pd based membrane by 80%. They also stated that ‘‘addition of

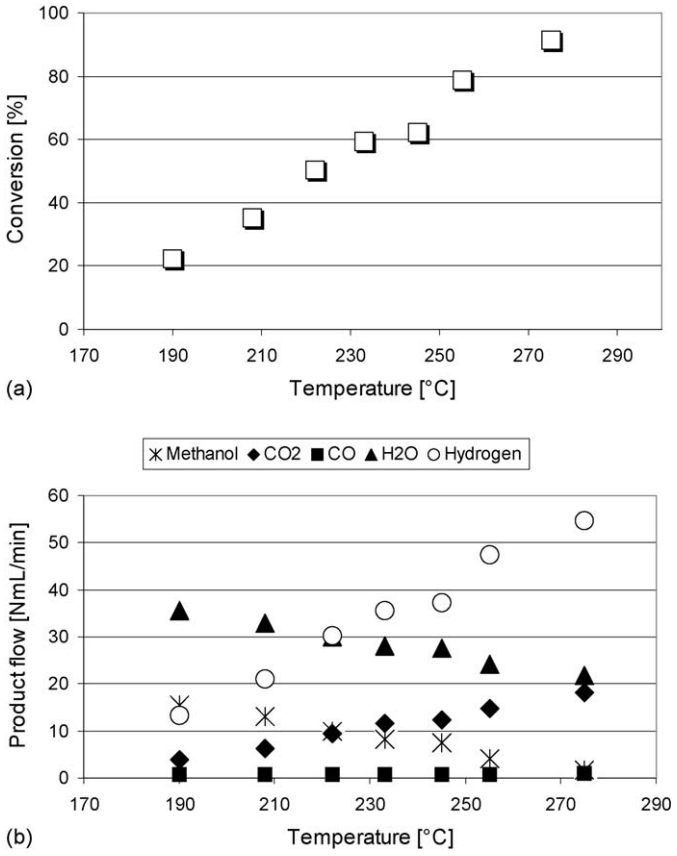

Fig. 4. Methanol conversion (a) and product composition (b) as a function of temperature during the methanol steam reforming over a 1.6 μm self-supported Pd/23 wt.% Ag membrane. MSR reactant composition as specified in Table 1.

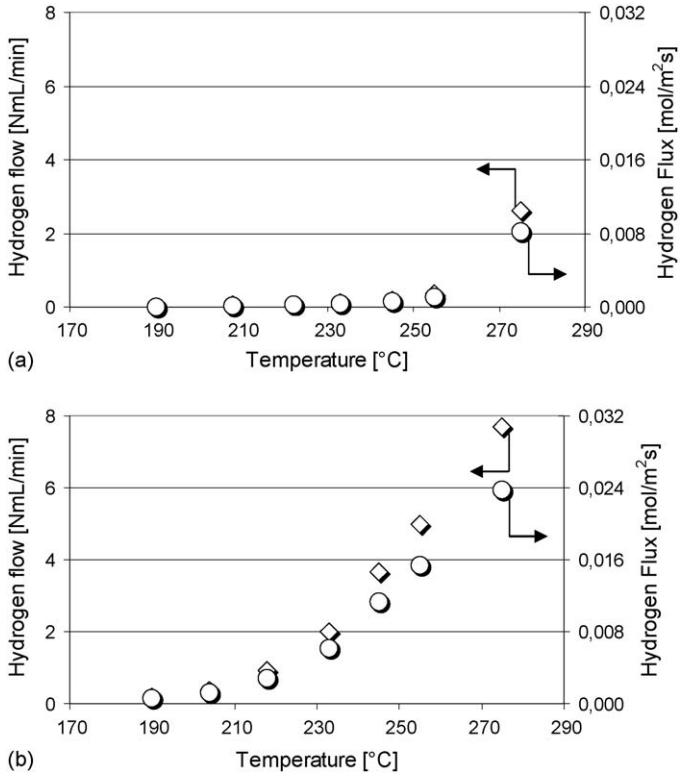

Fig. 5. Hydrogen permeation through the Pd/23 wt.% Ag membrane as a function of temperature during the first (a) and last (b) MSR experiments. MSR reactant composition as specified in Table 1. Conversion and product composition as in Fig. 4 for both experiments.

steam to such feeds can maintain the membrane performance by oxidising the deposits'' [45].

During the span of the MSR experimental period, the hydrogen flow rate through the membrane increased from one experiment to the next, under otherwise unchanged experimental conditions. Fig. 5(a) shows that there is a significant increase in the hydrogen permeation measured in the last reaction experiment. At the same time, there were no significant differences in the conversion and product composition between the first (Fig. 4) and last (not shown) MSR experiment. Possible errors or effects that could lead to this increased hydrogen permeation were checked carefully. No species except hydrogen and nitrogen (sweep gas) were detected on the permeate side during the MSR reaction. The hydrogen and nitrogen GC signal also excluded any reductions in the nitrogen sweep gas flow that could lead to erroneous interpretations. Hence, there is unequivocally an increase in the permeation, not explained by membrane failure or similar. The reason for the increased hydrogen permeation rate with MSR reaction time is so far not clear, but it could be that the nature of the adsorbed species changes, e.g. from large methanol molecules, or similar, to smaller CO, OH, etc. leaving the surface more open for hydrogen.

Between MSR reaction experiments, pure hydrogen permeation experiments were also carried out. In the pure hydrogen permeation experiment before the last MSR experiments, the flow through the membrane increased steadily from 39 NmL/min to 44 NmL/min during 5 h at 255 °C. These observations contrast with those between WGS reaction experiments, where the hydrogen permeation reached a constant value after 30–60 min. This may indicate that the membrane surface after exposure to MSR conditions is covered with species that react with atomic/molecular hydrogen on the surface and eventually disappears, albeit slowly. In analogy with the discussion above, a potential candidate could be adsorbed methoxy groups. At high hydrogen concentrations the methoxy groups can be hydrogenated to methanol that desorbs from the surface, thereby liberating hydrogen adsorption/dissociation sites.

When using the steel plate during MSR, the GC product analyses some times detected tiny amounts of methane, ~0.05 NmL/min at most. When the membrane was mounted, methane was detected less frequently and in lower amounts.

3.4. Membrane characterization

A wide scan X-ray photoelectron spectrum obtained at the retentate surface of the Pd/Ag membrane subjected to WGS reaction experiments is shown in Fig. 6. The dominant peaks are carbon 1s and oxygen Auger peaks, in addition to Ag and Pd 3p, 3d and Auger peaks. The corresponding spectrum obtained for the membrane used in MSR experiments is relatively similar, and is not shown. Table 4 shows the estimated surface composition of the WGS and MSR membranes after the experimental period, with corresponding analyses of an unused, as-grown membrane included. The estimated amount of C and O

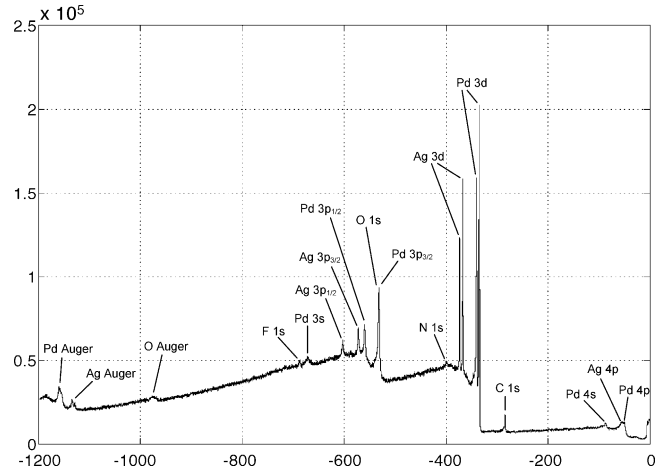

Fig. 6. Wide scan XPS spectrum of the Pd/23 wt.% Ag membrane subjected to WGS reaction experiments showing the surface composition of the membrane retentate side.

in the surface of the membranes subjected to the WGS or MSR reaction conditions is only slightly larger as compared to the corresponding unused membranes. This means that most of the carbon and oxygen originates from exposure to air before insertion into the XPS UHV chamber. Before the XPS analysis, the 3-days nitrogen flushing procedure was applied prior to two final days of WGS reaction experiments. This confirms that the previously described strongly adsorbed species deriving from CO accumulate slowly, and may support the idea that they are affiliated with special sites that are also essential to hydrogen activation transport through the membrane.

Neither does it appear that the conditions applied result in strong oxide growth on the surface, particularly because there is, if anything, rather a decrease than an increase in Ag level at

Table 4
Relative element composition of the Pd/23 wt.% Ag membrane surfaces as estimated from XPS analyses of the membrane retentate, correspondingly growth surface, side

Reaction	Relative % in the XPS signal			
	Pd 3d	Ag 3d	C 1s	O Auger
As-grown	36	16	25	23
WGS	34	12	26	29
MSR	35	12	27	26

the surface, the metallic species most likely to form oxides. XPS analyses estimated about 30 atomic% Ag in the surface of the unused membranes, i.e. an enrichment relative to the bulk composition. This is reduced to 25–26 atomic% Ag, a value nearer to the bulk composition, in the membranes subjected to the reaction mixtures.

Small amounts of nitrogen were also observed for both the WGS and MSR membrane surface. Nitrogen was not observed in the surface of the fresh, non-treated, membrane, meaning that nitrogen adsorbed from air is desorbed under evacuation. XPS measurements previously reported on similar Pd/Ag membranes subjected to activation in air also displayed a small nitrogen peak [48]. Hence, nitrogen appears to be ‘‘trapped’’ or bound to the surface upon exposure to air or nitrogen containing mixtures at elevated temperature. A tiny peak corresponding to F 1s was detected in the WGS membrane only (Fig. 6). A plausible explanation is a small contamination originating from an O-ring used in a sealing up-stream of the reactor. The O-ring is a polymer composed of polyvinylidene fluoride and hexafluoropropene monomers. The measurement is very sensitive to fluorine, hence it does not appear to have impact on the membrane performance. No traces of other metals that could stem from the catalyst or the reactor walls were detected.

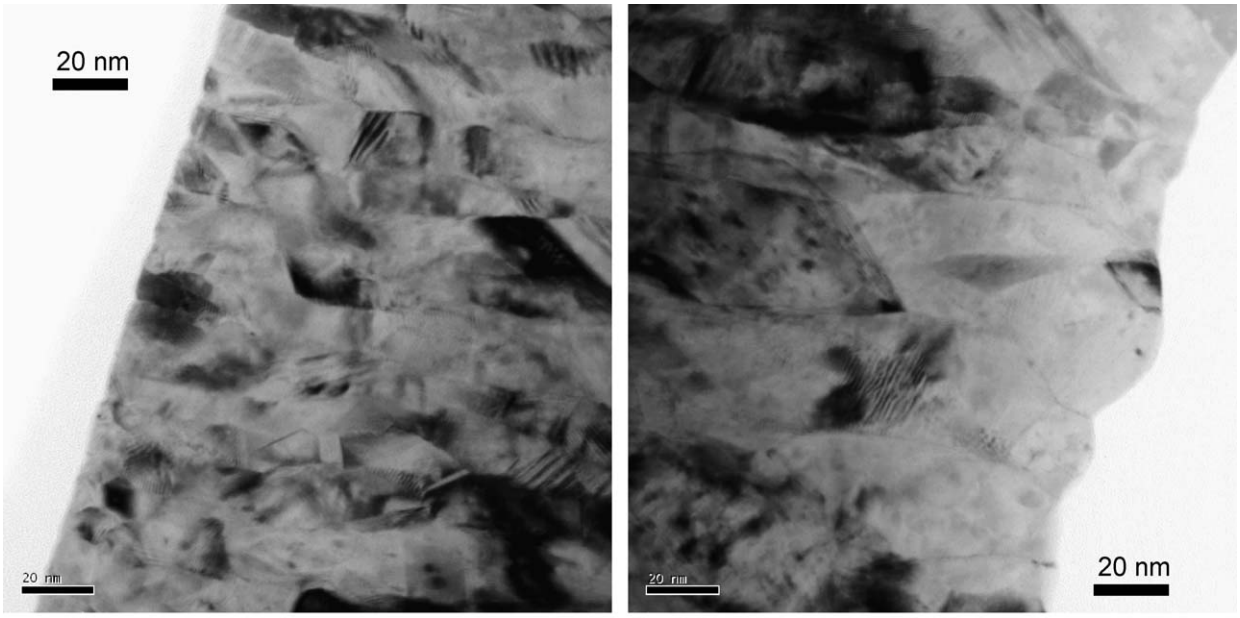

Fig. 7. Bright field TEM images obtained of from an as-grown, 1.3 μm Pd/23 wt.% Ag membrane: (a) region corresponding to the membrane/Si-substrate interface during growth; (b) region corresponding to the growth surface.

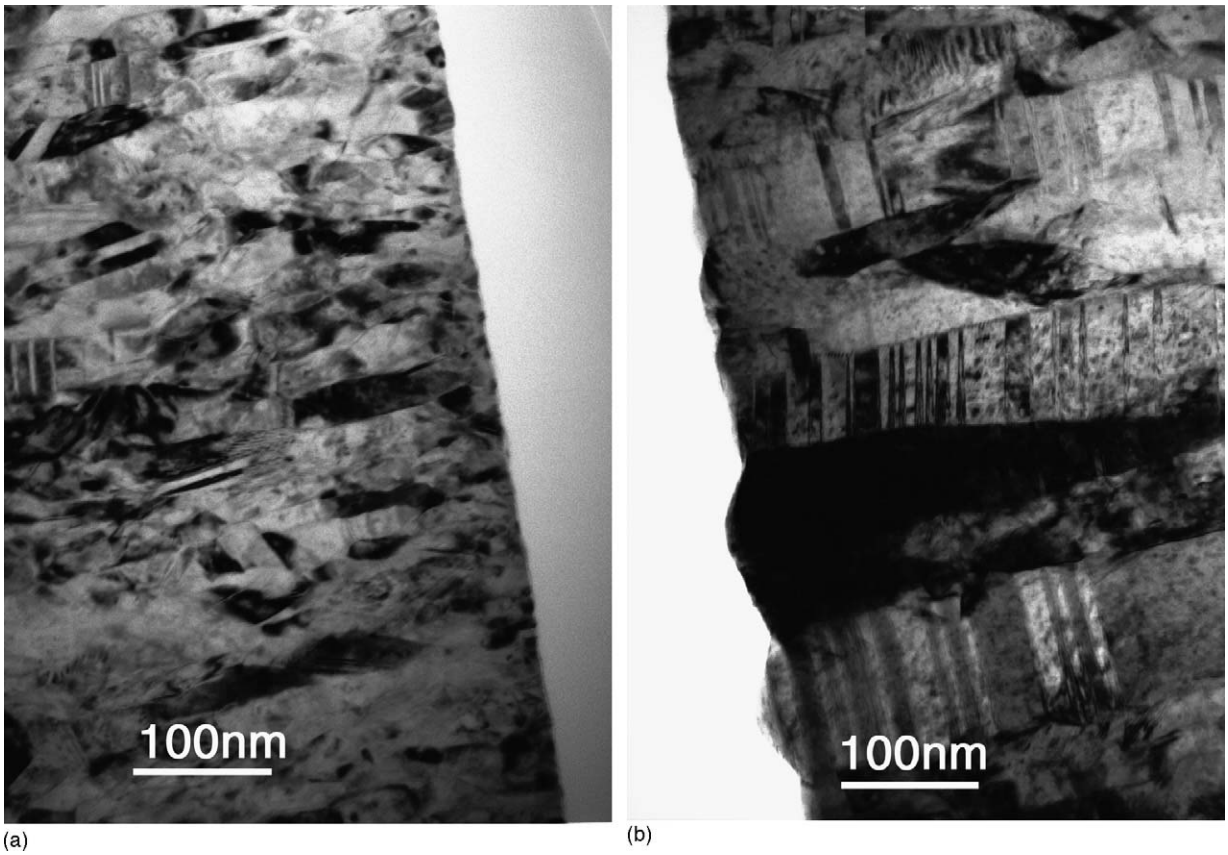

Fig. 8. Bright field TEM images obtained of from the 1.6 μm Pd/23 wt.% Ag membrane subjected to MSR reaction experiments: (a) region corresponding to the permeate side and the membrane/Si-substrate interface during growth; (b) region corresponding to the retentate side and the growth surface.

Fig. 7 shows bright field TEM images obtained from an as-grown, 1.3 μm Pd/23 wt.% Ag membrane. The images illustrate the grain structure of the membrane near the surface corresponding to the membrane/substrate (Si) interface during growth (a) and near the growth surface (b). The grain structure is observed to be columnar through the membrane, and coarsening with membrane thickness. The substrate side is characterized by small grains and a smooth surface (Fig. 7a). A mean grain width of 18 nm was estimated for the substrate side by measuring an average distance between grain boundaries crossing a straight line parallel to and approximately 100 nm below the surface. The growth surface is rougher (Fig. 7b) and the corresponding grain width estimated ∼100 nm below the growth surface is 39 nm. The growth direction appears to be (1 1 1), as indicated by the observation of planar defects such as twin lamellas in the grains. The twins are mainly found near the growth surface, and their traces are roughly parallel to the growth surface.

Fig. 8 show bright field TEM images obtained for the membrane subjected to MSR reaction conditions. Corresponding images obtained for the WGS membrane looked relatively similar, and are not shown. The images illustrate the grain structure on the permeate (a) and retentate (b) sides. It is important to note that the permeate side also corresponds to the membrane/substrate (Si) interface during growth, and that the retentate side corresponds to the growth surface. The most apparent difference, compared with the unused membrane, is that the grain size of the used membranes is larger. Table 5 summarizes the grain sizes in the three membranes.

An increase in grain size appears to link with improved hydrogen permeation properties for these membranes, but this is still under investigation. We are therefore not in a position to conclude whether this effect relates to bulk restructuring or surface roughening processes, or a combination. The change in the surface Pd/Ag ratio during reaction experiments as observed by XPS is also correlated to the grain growth and change in properties. In addition, any improved transport properties upon grain growth during WGS reaction experiments is counteracted by CO adsorption. Whether the surface roughening creates more sites for the fraction of strongly adsorbed CO species should be addressed.

The conclusion that the WGS and MSR exposed membranes are relatively similar, as examined by XPS and TEM, thus

Table 5
Average grain width as estimated by the average distance between grain boundaries crossing a straight line parallel to and approximately 100 nm below the surface for an as-grown membrane and for the two membranes used in the WGS and MSR experiments

Pd/23 wt.% Ag membrane (thickness)	Growth surface (retentate side) (nm)	Substrate-interfaced (permeate side) (nm)
As-grown (1.3 μm)	39	18
WGS (1.6 μm)	87	38
MSR (1.6 μm)	70	29

applies only to a certain extent and scale. The TEM investigations of the unused membranes showed that it is possible to image lattice defects, grain boundaries and phase distribution down to the atomic scale, albeit while suffering gradual electron beam damage. Such investigations can reveal which structural features on the nanometer scale are important for permeation and stability under realistic conditions. Also prolonged exposure to reaction conditions and high resolution photoelectron spectroscopy can reveal the nature of slowly accumulating species as well as more subtle variations in the chemical composition of the surface.

4. Conclusions

Self-supported Pd/23 wt.% Ag membranes of 1.6 μm thickness and 17 mm diameter were prepared and applied in membrane reactor experiments under water-gas shift and methanol steam reforming reaction conditions. Repeated WGS or MSR experiments could be performed over these extremely thin membranes, with permeation tests in between. The configuration was not optimised for conversion enhancement by shift of equilibrium towards the product side. Alternatively, the experimental set-up has allowed studies of the membrane properties without any effects of a porous mechanical support structure.

CO is found to have a deactivating effect on the hydrogen permeation, whereas the effect of steam is probably mainly attributed to dilution. The main effect of CO is competitive adsorption on the Pd/Ag surface. In addition, some CO or CO-derived species appear to be strongly, but not irreversibly, adsorbed. The accumulation of these CO-derived species causes a slow deactivation of the hydrogen permeation.

There is, furthermore, a significant reduction in hydrogen permeation upon exposure to the reactant/product mixtures, as compared to permeation experiments with pure hydrogen and inert gases. During WGS, this is attributable to the competitive adsorption of CO, which shows a strongly adsorbed component also here. The concentration of CO under MSR conditions is low, and the limited permeation is ascribable to adsorbed species derived from unconverted methanol. Repeated WGS reaction experiments lead to a continuous decline in hydrogen permeation, also under pure hydrogen exposure, which could only be restored by prolonged nitrogen flushing. In contrast, repeated MSR experiments continuously improved the hydrogen permeation also under reaction conditions.

XPS data showed that the main elements adsorbed on the surface were oxygen and carbon, as originating from exposure to air before insertion in the measurement chamber. In agreement with the reaction results, an irreversible build-up of oxide or carbonaceous species could be excluded. Strong contaminations originating from the catalyst or the reactor walls were not detected.

TEM investigations indicated that the grain width increased through both membranes during the reaction experiments, together with a roughening of the surface on the retentate side. The increasing grain size may enhance the transport properties of the membrane (both bulk diffusion and surface reaction rates), and this will be further studied. Why this is not observed during WGS may be due to the more efficient or strong site blocking of CO, as compared to methanol derived species, which dominate the overall permeation rate.

The self-supported, 1.6 μm Pd/23 wt.% Ag membranes show promising structural and chemical stability for use in a membrane reactor configuration for the production of 100% pure hydrogen by water-gas shift as well as the methanol steam reforming reactions. Successful implementation of low-thickness Pd-based membranes represents an important step towards reduced material expenses for future hydrogen separation technologies.

Acknowledgements

This work was supported by the Research Council of Norway through Grant No. 135938/431 (KOSK), 140022/V30 (RENERGI) and 158516/S10 (NANOMAT). Statoil ASA through the Gas Technology Center NTNU-SINTEF is also acknowledged for their support. The XPS analyses were performed by the photoemission laboratory headed by Professor Steinar Raaen at the Department of Physics, NTNU.

References

[1] R. Hughes, Membr. Tech. 131 (2001) 9.
[2] S.N. Paglieri, J.D. Way, Sep. Purif. Methods 31 (2002) 1.
[3] J. Armor, Catal. Today 25 (1995) 199.
[4] S. Uemiya, N. Sato, H. Ando, E. Kikuchi, Ind. Eng. Chem. Res. 30 (1991) 589.
[5] A. Basile, E. Drioli, F. Santella, V. Violate, G. Capanneli, G. Vitulli, Gas. Sep. Purif. 10 (1996) 53.
[6] A. Basile, A. Criscuoli, F. Santella, E. Drioli, Gas. Sep. Purif. 10 (1996) 243.
[7] A. Criscuoli, A. Basile, E. Drioli, Catal. Today 56 (2000) 53.
[8] A. Basile, G. Chiapetta, S. Tosti, V. Violante, Sep. Purif. Technol. 25 (2001) 549.
[9] S. Tosti, A. Basile, G. Chiappetta, C. Rizzello, V. Violante, Chem. Eng. J. 93 (2003) 23.
[10] S. Hara, W.-C. Xu, K. Sakai, N. Itoh, Ind. Eng. Chem. Res. 38 (1999) 488.
[11] Y.M. Lin, M.H. Rei, Int. J. Hydrogen Energy 25 (2000) 211.
[12] Y.M. Lin, M.H. Rei, Catal. Today 67 (2001) 77.
[13] N. Itoh, Y. Kaneko, A. Igarashi, Ind. Eng. Chem. Res. 41 (2002) 4702.
[14] A. Basile, F. Gallucci, L. Paturzo, Catal. Today 104 (2005) 244.
[15] A. Basile, F. Gallucci, L. Paturzo, Catal. Today 104 (2005) 251.
[16] B.A. Raich, H.C. Foley, Ind. Eng. Chem. Res. 37 (1998) 3888.
[17] J.N. Keuler, L. Lorenzen, Ind. Eng. Chem. Res. 41 (2002) 1960.
[18] W.H. Lin, H.F. Chang, Catal. Today 97 (2004) 181.
[19] J.N. Keuler, L. Lorenzen, J. Membr. Sci. 202 (2002) 17.
[20] E. Gobina, K. Hou, R. Hughes, J. Membr. Sci. 90 (1994) 11.
[21] E. Gobina, K. Hou, R. Hughes, Catal. Today 25 (1995) 365.
[22] E. Gobina, K. Hou, R. Hughes, Chem. Eng. Sci. 14 (1995) 2311.
[23] L.S. Wang, K. Murata, M. Inaba, Catal. Today 82 (2003) 99.
[24] J.P. Collins, R.W. Schwartz, R. Sehgal, T.L. Ward, C.J. Brinker, G.P. Hagen, C.A. Udovich, Ind. Eng. Chem. Res. 35 (1996) 4398.
[25] Y. Yildirim, E. Gobina, R. Hughes, J. Memb. Sci. 135 (1997) 107.
[26] H. Weyten, J. Luyten, K. Keizer, L. Willems, R. Leysen, Catal. Today 56 (2000) 3.
[27] M. Sheintuch, R.M. Dessau, Chem. Eng. Sci. 51 (1996) 535.
[28] T. Matsuda, I. Koike, N. Kubo, E. Kikuchi, Appl. Catal. A 96 (1993) 3.
[29] E. Kikuchi, Catal. Today 25 (1995) 333.
[30] T.M. Raybold, M.C. Huff, Catal. Today 56 (2000) 35.
[31] Y.L. Guo, G.Z. Lu, Y.S. Wang, R. Wang, Sep. Sci. Technol. 32 (2003) 271.
[32] W. Liang, R. Hughes, Catal. Today 104 (2005) 238.

[33] N. Itoh, T.H. Wu, J. Membr. Sci. 124 (1997) 213.
[34] A.M. Mondal, S. Ilias, Sep. Sci. Technol. 36 (2001) 1101.
[35] N. Itoh, E. Tamura, S. Hara, T. Takahashi, A. Shono, K. Satoh, T. Namba, Catal. Today 82 (2003) 119.
[36] P. Ferreira-Aparico, I. Rodriguez-Ramos, A. Guerrero-Ruiz, Chem. Comm. 18 (2002) 2082.
[37] J.K. Ali, A. Baiker, Appl. Catal. 155 (1997) 27.
[38] S. Uemiya, N. Sato, H. Ando, T. Matsuda, E. Kikuchi, Appl. Catal. 67 (1991) 223.
[39] S.L. Jørgensen, P.E.H. Nielsen, P. Lehrmann, Catal. Today. 25 (1995) 303.
[40] G. Barbieri, V. Violante, F.P. Di Maio, A. Criscuoli, E. Drioli, Ind. Eng. Chem. Res. 36 (1997) 3369.
[41] F. Gallucci, L. Paturzo, A. Fama, A. Basile, Ind. Eng. Chem. Res. 43 (2004) 928.
[42] J. Tong, Y. Matsumura, H. Suda, K. Haraya, Ind. Eng. Chem. Res. 44 (2005) 1454.
[43] P. Ferreira-Aparicio, M. Benito, K. Kouachi, S. Menad, J. Catal. 231 (2005) 331.
[44] R. Bredesen, H. Klette, US Patent 6,086,729. July 11, 2000.
[45] K. Hou, R. Hughes, J. Membr. Sci. 206 (2002) 119.
[46] H. Gao, Y.S. Lin, Y. Li, B. Zhang, Ind. Eng. Chem. Res. 43 (2004) 6920.
[47] H. Amandusson, L.-G. Ekedahl, H. Dannetun, Appl. Surf. Sci. 153 (2000) 259.
[48] H. Klette, A. Mejdell, A. Borg, H. Venvik, R. Bredesen, Activation of very thin Pd–Ag membranes, in: Proceedings of the 6th International Conference on Catalysis in Membrane Reactors, Lahnstein, Germany, 7–9 July, 2004 (oral presentation).